Synthesis of Poly(ε-caprolactone)/Clay Nanocomposites Using Polyhedral Oligomeric Silsesquioxane Surfactants as Organic Modifier and Initiator

Md. D. Hossain,[1] Youngjae Yoo,[2] Kwon T. Lim[1]

[1]*Division of Image and Information Engineering, Pukyong National University, Busan 608-739, Korea*
[2]*Department of Chemical Engineering, Texas Materials Institute, The University of Texas at Austin, Austin, Texas 78712*

Received 30 August 2009; accepted 12 May 2010
DOI 10.1002/app.32791
Published online 29 July 2010 in Wiley Online Library (wileyonlinelibrary.com).

ABSTRACT: Poly(ε-caprolactone)/clay nanocomposites were synthesized by *in situ* ring-opening polymerization of ε-caprolactone in the presence of montmorillonite modified by hydroxyl functionalized, quaternized polyhedral oligomeric silsesquioxane (POSS) surfactants. The octa(3-chloropropyl) polyhedral oligomeric silsesquioxane was prepared by hydrolytic condensation of 3-chloropropyltrimethoxysilane, which was subsequently quaternized with 2-dimethylaminoethanol. Montmorillonite was modified with the quaternized surfactants by cation exchange reaction. Bulk polymerization of ε-caprolactone was conducted at 110°C using stannous octoate as an initiator/catalyst. Nanocomposites were analyzed by X-ray diffraction, transmission electron microscopy, thermo gravimetric analysis, and differential scanning calorimetry. Hydroxyl functionalized POSS was employed as a surface modifier for clay which gives stable clay separation for its 3-D structure and also facilitates the miscibility of polymer with clay in the nanocomposites due to the star architecture. An improvement in the thermal stability of PCL was observed even at 1 wt % of clay loading. © 2010 Wiley Periodicals, Inc. J Appl Polym Sci 119: 936–943, 2011

Key words: caprolactone; montmorillonite clay; nanocomposites; ring opening polymerization; polyhedral oligomeric silsesquioxane

INTRODUCTION

In the past decade, polymer nanocomposites have emerged as a new class of materials and have received considerable attention as an effective method of enhancing thermal stability and flame retardant, mechanical, and barrier properties.[1–6] Montmorillonite, the most preferred and widely used smectic clay is of particular interest because it offers a high aspect ratio (10–1000) and a high surface area.[7] Due to an isomorphic substitution within the layers, the clay layer is negatively charged, which is counterbalanced by cations in the interlayer space.

The natural montmorillonite is hydrophilic and is generally considered unsuitable for hosting non-polar organic molecules without prior treatment. In addition, clay particles are composed of sheets that are stacked roughly 1 nm apart. The narrow spacing between the inorganic sheets inhibits the polymer permeation into the particles. Thus, the fabrication of thermodynamically stable composites where the clay sheets are uniformly dispersed (or exfoliated) within the polymer matrix poses significant synthetic challenges. Usually interlayer cations can be exchanged with organic cations to obtain organophilic montmorillonite producing an "organoclay," which has an expanded interlayer spacing and readily produces polymer/clay nanocomposites. Employing different organic cations (surfactants) could achieve different natures of morphologies of the nanocomposites: intercalated, intercalated and flocculated, and exfoliated.[8] It is well documented that exfoliated nanocomposites provide the best property enhancement due to the large aspect ratio and surface area of clay.[9] However, there are few unequivocal examples of the synthesis of exfoliated nanocomposites because the strong electrostatic force between clay layers tends to hold them together and underlie the preferred face-to-face stacking geometry in agglomerated clay tactoids.[10] In contrast, partially exfoliated nanocomposites are readily produced having silicate layers exfoliated into secondary particles which contain several stacked, coplanar layers. Two main approaches can be used to prepare polymer/clay nanocomposites: either melt-intercalation, for which clay is mixed with preformed polymers in the

Correspondence to: K. T. Lim (ktlim@pknu.ac.kr).
Contract grant sponsor: National Research Foundation (MEST): Korea Science and Engineering Foundation (KOSEF); contract grant number: R01-2008-000-21056-0, BK21 Program.

molten state, or *in situ* intercalative polymerization, where clay is dispersed in monomers which are subsequently polymerized. The *in situ* intercalative polymerization was shown to be the most efficient synthetic path since it allows the generation of completely exfoliated morphologies, leading to polymer/clay nanocomposites with much-improved properties.

During the last decade, an increasing attention has been paid to biodegradable polymers because of their sustainability. Poly(ε-caprolactone) (PCL) is a well known green polymer which can be prepared by ring opening polymerization (ROP) of ε-caprolactone in the presence of catalyst and initiator. However, the applications of such polymers are limited because of incompatibility in mechanical and barrier properties to water and gasses. To improve the properties of the biodegradable polymers particularly for use as packaging materials, one option is to incorporate environmentally acceptable fillers. In this regard, clay is a suitable filler because it is a naturally abundant mineral that is toxin free. It can be used as one of the components for food, medical, cosmetic, and health-care recipients.[7–13] Recently, biodegradable polymers reinforced by clay have been investigated,[14–20] and the crystallization behavior of PCL/nanoclay were studied in detail by melt processing.[21] A small amount of fillers particularly organically modified layered silicates improved the mechanical,[22–24] thermal[14,25,26] and gas barrier properties[16] of the matrix PCL. To synthesize PCL/clay nanocomposites with controlled PCL chain lengths and exfoliated structures, *in situ* ROP of ε-caprolactone with a well-controlled coordination/insertion mechanism has been used.[27–31] The ROP was catalyzed by tin(II) 2-ethylhexanoate, dibutyltin(IV) dimethoxide, or triethylaluminum in the presence of clay modified by quaternary ammonium cations containing hydroxyl groups. The hydroxyl groups can act as initiators for the ROP, yielding surface grafted PCL chains and leading to an exfoliated morphology. In exfoliated PCL/clay nanocomposites, the clay layers completely lose their stacking orders and are uniformly dispersed in the continuous PCL matrix. Such PCL/clay nanocomposites can attain a particular degree of properties with less clay content than that with the intercalated structures.[30]

In this work, we prepared poly(ε-caprolactone)/clay nanocomposites by *in situ* ring-opening polymerization of ε-caprolactone catalyzed by Tin(II) 2-ethylhexanoate in the presence of the clay modified by a 3-D surfactant, hydroxyl functionalized quaternized polyhedral oligomeric silsesquioxane (POSS). In addition, the thermal properties and crystallization behavior of the nanocomposites were investigated.

MATERIALS AND METHODS

Materials

Montmorillonite (MMT) (Morrisville, Pennsylvania) which has cation exchanged capacity of 92.6 meq/100 g was obtained from Gelest. 3-Chloropropyl trimethoxysilane (97+%), 2-dimethylaminoethanol (99.5+%), Tin(II) 2-ethylhexanoate (~99%) were purchased from Aldrich (Yongin, Korea) and were used without additional purification. ε-Caprolactone (Aldrich, Yongin, Korea) was dried over CaH_2 and distilled under reduced pressure prior to use.

Synthesis of octa (3-chloropropyl) poss

Octa(3-chloropropyl) POSS was synthesized by slight modification of the procedure reported elsewhere.[32] Typically, 3-chloropropyltrimethoxysilane (10 g, 0.05 mol), methanol (225 mL), and conc. HCl (10 mL of 35% in H_2O) were stirred at room temperature for 5 weeks. POSS-$(Cl)_8$ was obtained as white powder after suction filtration followed by washing with deionized water (3.2 g, yield: 32%). ^{1}H-NMR ($CDCl_3$, δ, ppm, TMS) assignment: 0.78–0.82 (2H, Si—CH_2), 1.85–1.91 (2H, Si—CH_2CH_2), 3.52–3.54 (2H, Si—$CH_2CH_2CH_2Cl$).

Synthesis of octa (2-hydroxyethyl dimethylaminopropyl) poss

Octa (2-hydroxyethyl dimethylaminopropyl) POSS was prepared by a quaternization reaction as depicted in Figure 1. Initially, octa(3-chloropropyl) POSS (1.0 g) was dissolved in a mixed solvent of ethanol (5 mL) and *N*,*N*-dimethyl formamide (2 mL) and reacted with 2-dimethylaminoethanol (0.8 mL) at 80°C for 2 days. After solvent evaporation, the reaction product was precipitated in *n*-hexane and recovered as white powder that was dried under vacuum at ambient temperature for 24 h. ^{1}H-NMR analysis showed that more than 95% of the 3-chloropropyl groups were transformed to quaternized ammonium groups. ^{1}H-NMR ($CDCl_3$, δ, ppm, TMS), assignment: 0.69–0.83 (2H, $SiCH_2$); 1.72–1.85 (2H, Si—CH_2CH_2); 3.07–3.1 (2H, Si—$CH_2CH_2CH_2$); 3.33–3.36 (6H, N $(CH_3)_2$); 3.36–3.45 (2H, NCH_2); 3.82–3.89 (2H, NCH_2CH_2); 3.76–3.80 (NCH_2CH_2OH).

Modification of MMT

Na-MMT (1.0 g) was dispersed in 50 mL of deionized water under vigorous stirring to form suspension. 0.5 g of the octa(2-hydroxyethyl dimethylaminopropyl) POSS surfactant was dissolved in 25 mL deionized water. The solution was then added to the aqueous suspension. The mixture was stirred for 24 h before it was collected by filtration. The solid precipitate was subsequently washed with water

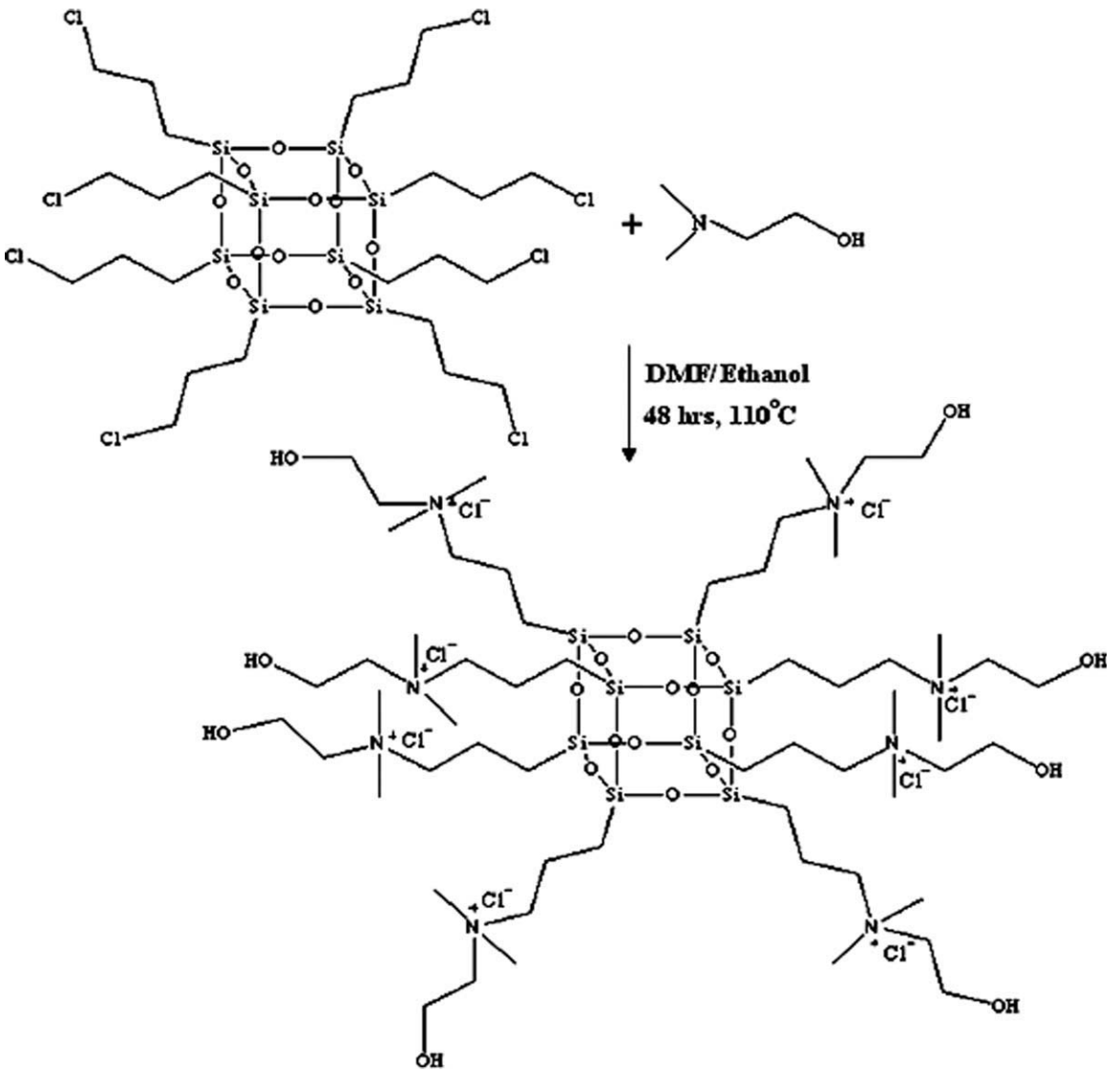

Figure 1 Synthesis of octa(2-hydroxyethyl dimethylaminopropyl) POSS.

several times until there was no white precipitate observed by adding 0.1 *M* $AgNO_3$, confirming the absence of chloride ions. The product was then vacuum-dried at 50°C for 48 h, grounded into powder, and stored in a desiccator. The modified clay was denoted as OMMT (organic montmorillonite).

Preparation of poly(ε-caprolactone)/clay nanocomposites

The desired amount of clay was placed in a polymerization vial and dried under vacuum at 60°C for 1 h. A known amount of ε-caprolactone and a solution of Tin(II) 2-ethylhexanoate in dry toluene were added into the vial. The $[monomer]_0/[Sn]$ molar ratio was 300. The reaction medium was then sonicated for 30 min and nitrogen gas was passed through the solution for another 30 min. Finally, the polymerization was allowed to proceed at 110°C for 24 h under nitrogen atmosphere. The product was diluted with a small amount of CH_2Cl_2 and precipitated in excess amount of *n*-hexane. After filtration, the PCL/clay composites were dried in a vacuum oven at 40°C for 48 h. The yield was calculated gravimetrically.

Characterization

^{1}H-NMR spectra were recorded using a JNM-ECP 400 (JEOL). The degree of quaternization of the QPSSQ surfactant was determined by ^{1}H-NMR spectra in $CDCl_3$ solvent. Powder X-ray diffraction (XRD) data were collected on a Philips X'pert MPD diffractometer using Cu Kα radiation. The XRD patterns were recorded in the range of 1°–10° at a scanning rate of 1° min^{-1} and 10°–50° using step scanning mode with the step size of 0.02° and the preset time of 0.5 s. Transmission electron microscopy

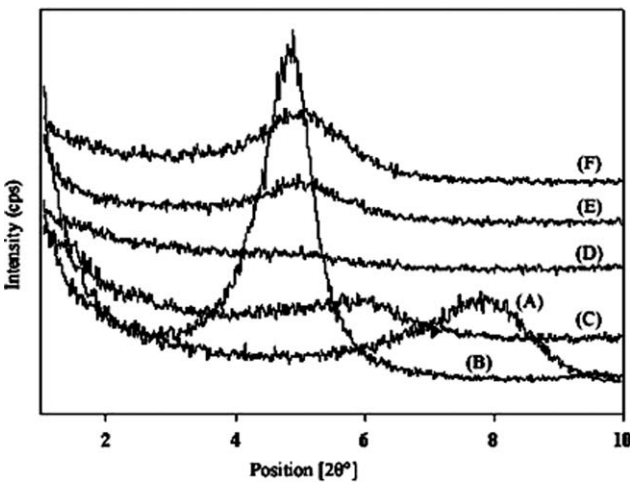

Figure 2 XRD patterns of (A) Na-MMT, (B) organic MMT, (C) MMT/PCL nanocomposites with 5 wt % Na-MMT, (D) MMT/PCL nanocomposites with 1 wt %, (E) 5 wt %, and (F) 10 wt % of organic MMT.

(TEM; JEOL 2010F, operating under an accelerating voltage of 120 kV) were used to observe the morphologies and microstructures of the nanocomposites. Samples for morphology analyzes were taken from the core portion of an injection-molded bar. Ultra-thin sections of ~50 nm thicknesses were cryogenically cut with a diamond knife while cooled using liquid nitrogen at a temperature of −80°C using an RMC PowerTome XL microtome. These sections were taken from the plane defined by the flow direction (FD) and the normal direction (ND) of the molded bar as explained elsewhere.[33] Sections were collected using 300 mesh grids and dried using filter paper. Thermo gravimetric analysis (TGA) was performed using a Perkin Elmer TGA-7 system in air atmosphere from room temperature to 600°C at a heating rate of 20°C min^{-1}. Differential scanning calorimetry (DSC) has been used to study the crystallization kinetics of the PCL intercalated chains in the nanocomposites. The measurements have been conducted with a Perkin Elmer Pyris 1 DSC instruments calibrated with indium. Samples were encapsulated in aluminum pans and the following cycle has been used: heated at 10°C/min from room temperature to 100°C, held at 100°C for 5 min and then cooled at 10°C/min to −50°C and finally heated to 100°C at 10°C/min. Measurements have been performed twice and enthalpy values were reproducible within 5%.

RESULTS AND DISCUSSION

Poly(ε-caprolactone)/clay nanocomposites with 5 wt % of pristine clay (Na-MMT) and 1, 5, and 10 wt % of the organic clay were prepared by the polymerization of ε-caprolactone in bulk at 110°C by Tin(II) 2-ethylhexanoate. Small angle X-ray diffraction (XRD) was used to characterize the layered structure of the polymer/clay nanocomposites. Figure 2 shows the XRD patterns of sodium montmorillonite, organic clay, poly(ε-caprolactone)/clay nanocomposites with 5 wt % of Na-MMT and 1, 5, and 10 wt % of organic clay loadings. By using Bragg equation, the *d* (001) spacing values of the samples were calculated and used to characterize the layered structure of the polymer/clay nanocomposites. As is seen from curves in Figure 2(A,B), the *d*-spacing was expanded after the cation exchange with quaternized POSS surfactant from 11.8 Å to 18.16 Å. In the curve in Figure 2(C), the appearance of the peak at $2\theta = 5.19^\circ$ in the XRD pattern reveals the formation of partially intercalated nanocomposites by 5 wt % of Na-MMT clay loading. However, the complete disappearance of the peak in Figure 2(D) was observed for PCL/MMT nanocomposites synthesized using 1 wt % of organic clay loading. Although the disappearance of the reflection peak indicated a disordered structure, this did not provide enough information about whether the clay platelets were fully exfoliated and evenly dispersed throughout the polymer matrix. The peak intensity increased slightly with an increase in clay loading as shown in Figure 3(E,F) with 5 and 10 wt % of organic clay loadings. These results suggested that partially exfoliated nanocomposites were formed when the polymerization was conducted with higher clay loadings. The characteristic data for PCL and PCL/MMT nanocomposites synthesized with different clay loadings are given in Table I. All the polymerization resulted in high yields above 94%. The TEM analysis allowed direct visualization of the morphology, spatial distribution, and dispersion of the nanoparticles and platelets within the polymer matrix. In Figure 3, TEM images were shown to observe the microstructures of the nanocomposites, where the dark line represents individual silicate layers and the brighter area stands for the PCL matrix. When the polymerization was conducted using 1 wt % of organic clay loading, more exfoliated nanocomposites along with some intercalated clay tactoids were observed [Fig. 3(A)]. However, an increase in clay loading in the nanocomposites shows frustrated filling behavior,

TABLE I
Characteristic Data of PCL Homopolymer and PCL/MMT Nanocomposites with Different Clay Loadings

Sample code	Filler content (%)	Polymerization yield (%)	*d*-spacing (Å)
PCL	0	98.5	–
MP-5	5	95.73	14.94
OMP-1	1	97.97	Partially exfoliated
OMP-5	5	95.22	18.71
OMP-10	10	94.76	18.14

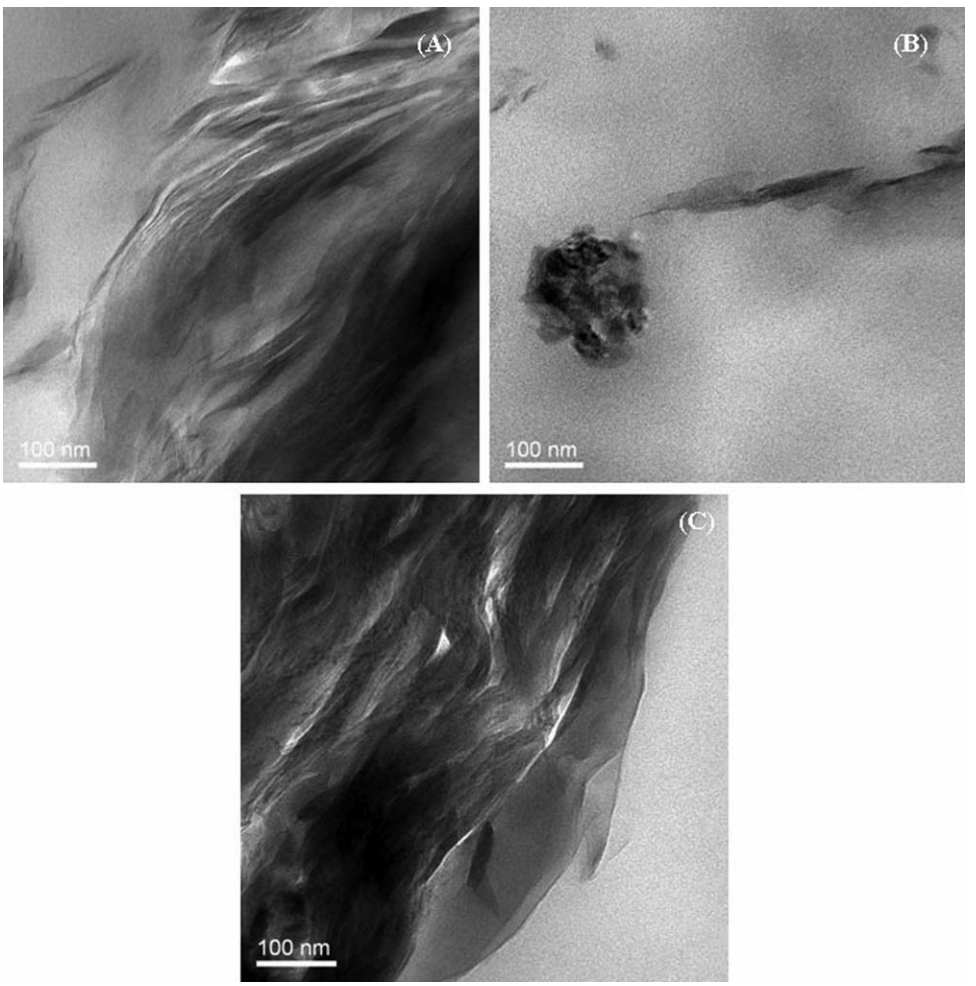

Figure 3 TEM images of PCL/MMT nanocomposites with (A) 1, (B) 5, and (C) 10 wt % of organic clay loadings.

where nanocomposites with agglomerated clay tactoids were formed. These results suggested that a small amount of clay loading might form exfoliated nanocomposites while higher clay loading shows unintercalated nanocomposites. Singh and Balazs have studied the influence of the architecture of polymers on the miscibility of polymer/clay nanocomposites. In their study, they used self-consistent field theory to predict that star-shaped polymers might form thermodynamically stable exfoliated clay nanocomposites.[34] However, our work in this field is to test the miscibility of clay with star polymer which was synthesized *in situ* and possibly realize an improvement in physical properties of the resulting nanocomposites. Our experimental results suggested that the star polymer which was synthesized *in situ* enhanced physical properties of the nanocomposites by incorporation of even 1 wt % of the nanoclay. Presumably, the relatively compact size of the star polymer combined with the multiple points of interaction with the surfactant-covered surface of the clay promotes the miscibility of the nanocomposites.[35]

Thermal degradation behavior of the nanocomposites was studied by TGA, heating from room temperature to 600°C at a rate of 20°C/min. In general, the thermal stability of the polymer/clay nanocomposites can be affected by polymer matrix, fillers, and the interaction between polymer matrix and fillers. Figure 4 shows that the nanocomposites with different clay loading degrade at higher temperature than neat PCL. This beneficial effect can be explained by a decrease in the diffusion of oxygen and volatile products throughout the composite material. However, the thermal degradation temperatures of the nanocomposites with different organic clay loadings were very close to each other, and no significant trend with increasing clay content was observed. An increase in the thermal degradation temperatures of the nanocomposites with increasing clay content has been generally observed for intercalated nanocomposites.[14,31,36] The reason may be related to the loss of thermal mobility and the heat transfer ability of chains confined between the platelets. In this case, the nanocomposites synthesized

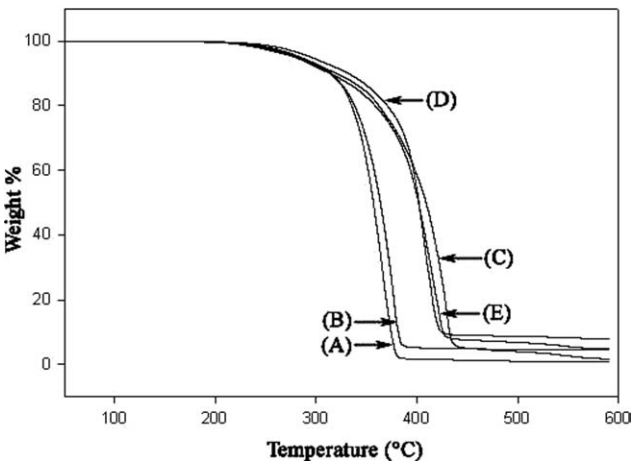

Figure 4 Temperature dependence of the weight loss for (A) pure PCL, (B) PCL/clay nanocomposites with 5 wt % of Na-MMT, (C) PCL/clay nanocomposites with 1 wt %, (D) 5 wt %, and (E) 10 wt % of organic clay (heating rate 20°C/min).

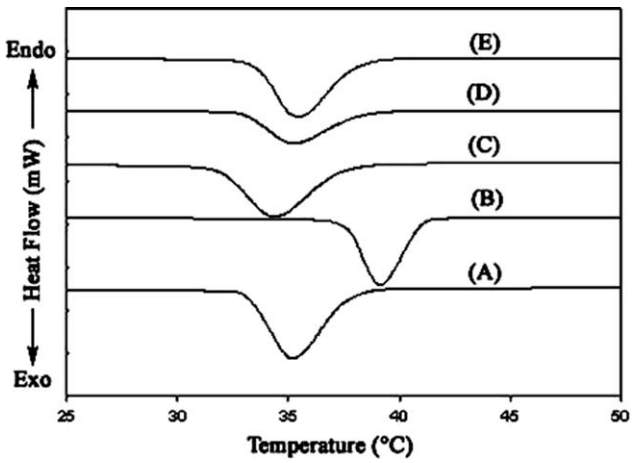

Figure 5 The DSC analysis on (A) PCL; PCL/MMT nanocomposites with (B) 5 wt % of NaMMT, (C) 1, (D) 5, and (E) 10 wt % of organic clay loadings, cooling step.

using 1 wt % of clay loading shows higher degradation temperature than that of the nanocomposites with higher clay loadings, due to its partially exfoliated nanostructure, which restrict thermal behavior or molecular mobility. It is observed from Figure 4(C) that the temperature at which 50% weight loss is shifted by 50°C towards higher temperature upon the addition of this clay loading. Higher amount of clay is, however, a little bit unfavorable as exemplified by temperature shift of 40°C when the content of organo-modified clay is 5 and 10 wt %. The nanocomposites using 5 wt % of Na-MMT did not show any significant heat change due to its partial intercalation of polymer into clay gallery. The TGA results were summarized in Table II and provide information on the degradation pathway of these materials. T_{25} and T_{50} represent the temperatures at which 25 and 50% degradation occur, respectively. The percentage, $W_{\%res}$ stands for residue that is not volatilized at 450°C. At the 1 wt % of clay content, relatively higher percentage of residue was found at 450°C temperature compared to higher clay contents. The thermal properties of the nanocomposites and PCL were further investigated by DSC. Both melting and crystallization processes of PCL were detected in the cooling and heating thermograms (Figs. 5 and 6) of the nanocomposites, which indicated that clay or POSS has significant effect on crystallization and melting of the polymer chains. The incorporation of 5 wt % of Na-MMT resulted in a significant increase of crystallization temperature (T_c), because Na-MMT acts as a nucleating agent which accelerate the crystallization of PCL.[37,38] The nanocomposites with 1 wt % of organic clay resulted in a slight decrease of crystallization temperature compared with neat PCL due to the restriction in the mobility of polymer chains caused by dispersed silicate nanolayers.[39] This can be attributed to the exfoliated structure of the nanocomposites with 1 wt % of organic clay. However, the crystallization temperature of the nanocomposites with 5 and 10 wt % of organic clay were similar with that of pure PCL, suggesting the nucleating and restriction effects are offset. On the other hand, the nanocomposites with Na-MMT and neat PCL displayed a similar melting transition at ca. 55.4°C, but the melting temperature slightly increased with the addition of modified clay by 0.4–0.7°C [Fig. 6(C–E)]. Liu et al. have shown that the star PCL displayed the higher melting temperature than their linear counterparts.[40] Furthermore, Singh and Balazs also explained that star-shaped polymer formed thermodynamically stable exfoliated nanocomposites.[34] These are in good agreement with our experimental results. The DSC results were summarized in Table III. The melting and crystallizing enthalpies (ΔH_c and ΔH_m, respectively) have been measured for each curve, and the PCL crystallinity degree has been deduced from these values, by using the formula $X_{PCL} = \Delta H \times W_{PCL}/\Delta H_o$, with X_{PCL} being the polycaprolactone crystallinity degree, W_{PCL} the weight fraction of the polyester, and ΔH_o the value for a 100% crystalline PCL, which is 136.1 J/g.[41] When comparing ΔH_c and ΔH_m values of the nanocomposites and neat PCL, the ΔH_c value is

TABLE II
TGA Data for PCL and PCL/MMT Nanocomposites Synthesized with Different Clay Loadings

Samples	T_{25} (°C)	T_{50} (°C)	$W_{\%\ res}$ (450°C)
PCL	340	357	1.28
MP-5	344	363	4.86
OMP-1	373	409	5.04
OMP-5	371	401	7.59
OMP-10	381	402	9.02

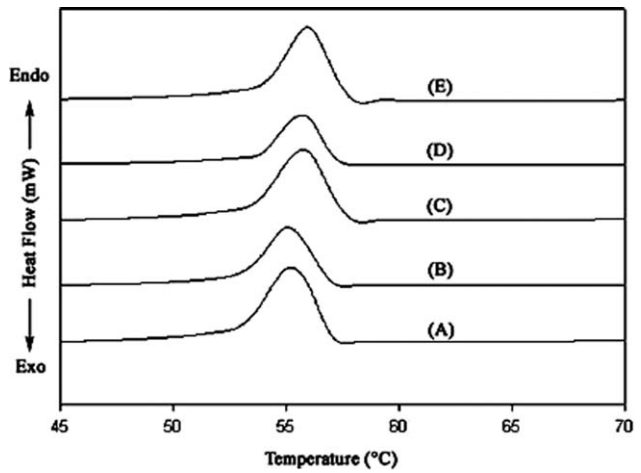

Figure 6 The DSC analysis on (A) PCL; PCL/MMT nanocomposites with (B) 5 wt % of Na-MMT, (C) 1, (D) 5, and (E) 10 wt % of organic clay loadings, second heating step.

higher for PCL/clay nanocomposites with 1 wt % of organic clay, but lower for 5 and 10 wt % of organic clay. Conversely, the ΔH_m values decreased significantly with the incorporation of the clay in the nanocomposites. This may be due to a melt–recrystallization–melt cycle during sample heating that reduces the real values for the melting enthalpy. This phenomenon had already been described by several authors when PCL was blended with amorphous polymers, such as SAN,[42] chlorinated polyethylene,[43] poly-(hydroxy ether of bisphenol A),[44] or poly(styrene-co-maleic anhydride).[45] A PCL double melting peak was observed during DSC analysis of the different polymer blends, whereas the pure PCL had a single melting peak. This reflects the strong effect of partial PCL grafting on its crystalline behavior, which favors the melt–recrystallization–melt cycle. The thermal properties of PCL/MMT nanocomposites were specifically investigated by Pucciarieollo et al.[46] Their results showed that the presence of organophilic clay increased the degree of crystallinity of PCL when the nanocomposites were exfoliated, but reduced the degree of crystallinity when the nanocomposites were intercalated. In this study, exfoliation of 1 wt % organic clay throughout the PCL matrix increased the degree of crystallinity of PCL. However, the increased content of organic clay to 5 and 10 wt % led to a decrease of crystallinity probably due to the partial intercalation of polymer inside clay galleries.

The wide-angle X-ray diffraction (WAXRD) measurements between 10° and 50° were also employed to examine the crystalline structure of PCL/clay nanocomposites, which are shown in Figure 7. For comparison, the diffraction pattern of PCL homopolymer was also incorporated in the figure. The diffraction peak positions of PCL homopolymer agree well with the reported unit cell parameters for PCL (orthorhombic, $a = 7.47$ Å, $b = 4.98$ Å, $c = 17.05$ Å).[47] The intense diffraction peaks located at $2\theta = 21.39°$, 22.00°, 23.70°, corresponding to the (110), (111), and (200) reflections were observed for the PCL. For the PCL/clay nanocomposites, it is seen that the diffraction peaks at $2\theta = 21.39°$, 22.00°, and 23.70° remained invariant in comparison with the PCL homopolymer. This observation suggests that there is little change in the crystalline structures. Therefore, the presence of clay in the PCL nanocomposites did not alter the packing structure of PCL chains in the crystals.[48–50]

CONCLUSIONS

A series of PCL/MMT nanocomposites have been prepared by *in situ* ROP of ε-caprolactone initiated by Tin(II) 2-ethylhexanoate in the presence of clay modified by the hydroxyl functionalized quaternized POSS. Partially exfoliated nanocomposites have been obtained when polymerization was conducted with 1 wt % of organic clay loading. However, with increasing the clay loading to 5 and 10 wt %, the degree of exfoliation of the nanocomposites decreased, which was assessed by both XRD and TEM analysis. From TGA, an improvement in the thermal stability of PCL was noted even at 1 wt % of clay loading. DSC analysis showed that the crystallization behavior of the nanocomposites with Na-MMT is significantly different from the composites with organic clay. While Na-MMT increases the crystallization temperature, a decrease in crystallization temperature was observed for the nanocomposites with 1 wt % of organic clay. All the nanocomposites displayed almost similar melting transition with that of neat PCL. The wide-angle X-ray scattering analysis also revealed that PCL/MMT

TABLE III
Enthalpy and Corresponding Crystallinity Values Obtained from the DSC Analysis

Sample	ΔH_c (J/g)	Crystanillity (%)	ΔH_m (J/g)	Crystanillity (%)	$\Delta H_c - \Delta H_m$ (J/g)
PCL	68.50	50.33	88.52	50.32	−20.02
MP-5	69.74	48.68	65.68	60.35	4.06
OMP-1	70.73	51.45	67.98	49.45	2.75
OMP-5	65.86	45.97	64.16	44.79	1.7
OMP-10	57.86	38.26	61.10	40.40	−3.24

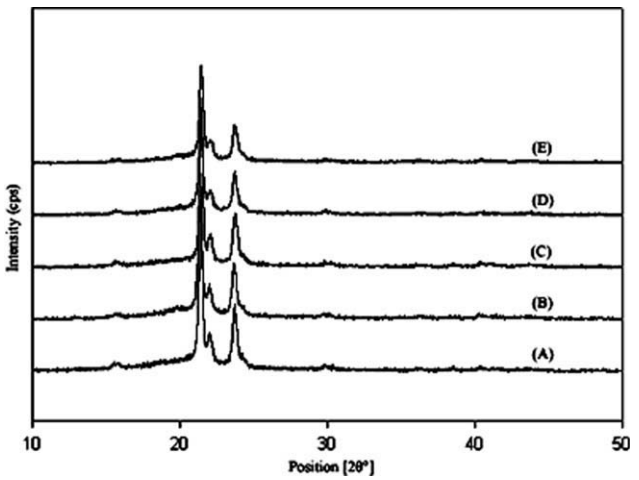

Figure 7 Wide angle XRD patterns of (A) PCL homopolymer; PCL/MMT nanocomposites with (B) 5 wt % of NaMMT, (C) 1, (D) 5, and (E) 10 wt % of organic MMT.

nanocomposites possessed crystalline structure even with high clay loading.

References

1. Zeng, Q. H.; Yu, A. B.; Lu, G. Q. (Max); Paul, D. R. J Nanosci Nanotech 2005, 5, 1574.
2. Gilman, J. W.; Jackson, C. L.; Morgan, A. B.; Harris, R. H.; Manias, E.; Giannelis, E. P.; Wuthernow, M.; Hilton, D.; Phillips, S. Chem Mater 2000, 12, 1866.
3. Wang, L. Q.; Liu, J.; Exarhos, G. J.; Flanigan, K. Y.; Bordia, B. J Phys Chem B 2000, 104, 2810.
4. Zhao, J.; Morgan, A. B.; Harris, J. D. Polymer 2005, 46, 8641.
5. Garces, J. M.; Moll, D. J.; Bicerano, J.; Fibiger, R.; Mcleod, D. G. Adv Mater 2000, 12, 1835.
6. Chen, B.; Evans, J. R. G.; Greenwell, H. C.; Boulet, P.; Coveney, P. V.; Bowden, A. A.; Whiting, A. Chem Soc Rev 2008, 37, 568.
7. Komori, Y.; Kuroda, K. Polymer-Layered Silicate Nanocomposites; Pinnavaia, T. J., Beall, G. W., Eds.; Wiley: West Sussex, UK, 2000; Vol. 1, pp 3–18.
8. Ray, S. S.; Okamoto, K.; Okamoto, M. Macromolecules 2003, 36, 2355.
9. Zeng, C.; Lee, L. J. Macromolecules 2001, 34, 4098.
10. Qian, Z.; Edward, T. S. Macromolecules 2005, 38, 7967.
11. Jinadasa, K. B. P. N.; Dissanayake, C. B. Environ Geochem Health 1992, 14, 3.
12. Bakraji, E. H.; Karajou, J. J. Trace Microprobe Tech 2003, 2, 397.
13. Pang, J. T.; Fan, C. H.; Liu, X. J.; Chen, T.; Li, G. X. Biosens Bioelectron 2003, 19, 441.
14. Lepoittevin, B.; Devalckenaere, M.; Pantoustier, N.; Alexandre, M.; Kubies, D.; Calberg, C.; Jerome, R.; Dubois, P. Polymer 2002, 43, 4017.
15. Gorrasi, G.; Tortora, M.; Vittoria, V.; Galli, G.; Chiellini, E. J Polym Sci Part B: Polym Phys 2002, 40, 1118.
16. Gorrasi, G.; Tortora, M.; Vittoria, V.; Pollet, E.; Lepoittevin, B.; Alexandre, M.; Dubois, P. Polymer 2003, 44, 2271.
17. Tortora, M.; Vittoria, V.; Galli, G.; Ritrovati, S.; Chiellini, E. Macromol Mater Eng 2002, 287, 243.
18. Chen, B.; Evans, J. R. G. Carbohydr Polym 2005, 61, 455.
19. Chen, M.; Chen, B.; Evans, J. R. G. Nanotechnology 2005, 16, 2334.
20. Ray, S. S.; Yamada, K.; Okamoto, M.; Fujimoto, Y.; Ogami, A.; Ueda, K. Chem Mater 2003, 15, 1456.
21. Homminga, D.; Goderis, B.; Dolbnya, I.; Groeninckx, G. Polymer 2006, 47, 1620.
22. Luduena, L. N.; Alvarez, V. A.; Vazquez, A. Mater Sci Eng A 2007, 460, 121.
23. Saeed, K.; Park, S. Y.; Lee, H. J.; Baek, J. B.; Huh, W. S. Polymer 2006, 47, 8019.
24. Chen, B.; Evans, J. R. G. Macromolecules 2006, 39, 747.
25. Chrissafis, K.; Antoniadis, G.; Paraskevopoulos, K. M.; Vassiliou, A.; Bikiaris, D. N. Compos Sci Technol 2007, 67, 2165.
26. Wu, Z.; Yin, J.; Yan, S.; Xie, Y.; Ma, J.; Chen, X. Polymer 2007, 48, 6439.
27. Kubies, D.; Pantoustier, N.; Dubois, P.; Rulmont, A.; Jerome, R. Macromolecules 2002, 35, 3318.
28. Lepoittevin, B.; Pantoustier, N.; Alexander, M.; Calberg, C.; Jerome, R.; Dubois, P. J Mater Chem 2002, 12, 3528.
29. Lepoittevin, B.; Pantoustier, N.; Devalckenaere, M.; Alexandre, M.; Kubies, D.; Calberg, C.; Jerome, R.; Dubois, P. Macromolecules 2002, 35, 8385.
30. Pantoustier, N.; Lepoittevin, B.; Alexandre, M.; Kubies, D.; Calberg, C.; Jerome, R.; Dubois, P. Polym Eng Sci 2002, 42, 1928.
31. Lepoittevin, B.; Pantoustier, N.; Devalckenaere, M.; Alexandre, M.; Calberg, C.; Jerome, R.; Henrist, C.; Rulmont, A.; Dubois, P. Polymer 2003, 44, 2033.
32. Chojnowski, J.; Fortuniak, W.; Rosciszewski, P.; Werel, W.; Lukasiak, J.; Kamysz, W.; Halasa, R. J Inorg Organomet Polym Mater 2006, 16, 219.
33. Yoon, P. J.; Fornes, T. D.; Paul, D. R. Polymer 2002, 43, 6727.
34. Singh, C.; Balazs, A. C. Polym Int 2000, 49, 469.
35. Robello, D. R.; Yamaguchi, N.; Blanton, T.; Barnes, C. J Am Chem Soc 2004, 126, 8118.
36. Lim, S. T.; Hyun, Y. H.; Choi, H. J.; Jhon, M. S. Chem Mater 2002, 14, 1839.
37. Kiersnowski, A.; Piglowski, J. Eur Polym J 2004, 40, 1199.
38. Wu, T.; Xie, T.; Yang, G. Appl Clay Sci 2009, 45, 105.
39. Urbanczyk, L.; Calberg, C.; Stassin, F.; Alexandre, M.; Jerome, R.; Jerome, C.; Detrembleur, C. Polymer 2008, 49, 3979.
40. Liu, Y.; Yang, X.; Zhang, W.; Zheng, S. Polymer 2006, 47, 6814.
41. Pucciariello, R.; Villani, V.; Gorrasi, G.; Vittoria, V. J Macromol Sci Phys 2005, 44, 79.
42. Rim, P. B.; Runt, J. P. Macromolecules 1983, 16, 762.
43. Defieuw, G.; Groeninckx, G.; Reynaers, H. Polymer 1989, 30, 595.
44. Defieuw, G.; Groeninckx, G.; Reynaers, H. Polymer 1989, 30, 2164.
45. Defieuw, G.; Groeninckx, G.; Reynaers, H. Polymer 1989, 30, 2158.
46. Pucciarieollo, R.; Villani, V.; Belviso, S.; Gorrasi, G.; Tortora, M.; Vittoria, V. J Polym Sci Part B: Polym Phys 2004, 42, 1321.
47. Hu, H.; Dorset, D. L. Macromolecules 1990, 23, 4604.
48. Chen, E. Q.; Lee, S. W.; Zhang, A.; Moon, B. S.; Man, I.; Harris, F. W. Macromolecules 1999, 32, 4784.
49. Floudas, G.; Reiter, G.; Lambert, O.; Dumas, P. Macromolecules 1998, 31, 72749.
50. Zhao, Y. L.; Cai, Q.; Jiang, J.; Shuai, X. T.; Bei, J. Z.; Chen, C. F. Polymer 2002, 43, 5819.